World Applied Sciences Journal 8 (3): 309-314, 2010
ISSN 1818-4952


# New Seismotectonic Aspects of East-Central Iran

[1]Ahmad Zamani and [1,2]Behzad G. Zamani

[1]Department of Geosciences, Faculty of Sciences, University of Shiraz, Iran
[2]Department of Geology, Faculty of Natural Sciences, University of Tabriz, Iran

**Abstract:** We study the state of stress in the East-Central Iran, based on systematic inversion of some available focal mechanisms of earthquakes. We have done stress inversion of double couple focal mechanisms of earthquakes recorded in the last century in the East-Central Iran. The calculated average stress regime in this area indicates major N62°E trending compression expressed in reverse and strike-slip focal mechanisms. This analysis show, the dominating tectonic regime in East-Central Iran is thrusting with a minimum stress axis, $\sigma_3$, close to vertical. As the difference between principal stresses $\sigma_2$ and $\sigma_3$ is minor with respect to the largest compressive stress, $\sigma_1$, this result is compatible with the presence of active strike-slip fault zones. This reconstruction of the seismotectonic stress in the East-Central Iran, with a NE-SW average trend of compression is consistent with independent information about the active plate convergence in Iran, related to Arabia-Eurasia convergence. Most earthquakes in this area occur near or around concealed Quaternary thrust faults, their activity being controlled by the NE-SW compression.

**Key words:** Seismotectonics · Stress · East-Central Iran · Focal mechanisms · Inversion

## INTRODUCTION

Iran is one of the countries, located within the convergence domain between the Arabian and Eurasian plates, which provides a relatively compact example of a young continent-continent collision zone. In Iran, Shortening is mainly accommodated by distributed faulting in high mountains of the Zagros in the south and the Alborz and Kopeh Dagh in the north. Eastern Iran is a region of widespread active faulting and right-lateral shear is taken up on several north-south right-lateral fault systems [1]. In the north, the right-lateral shear is seen as clockwise rotation about vertical axes of east-west left-lateral faults (the Doruneh and Dasht-e-Bayaz faults). Our study area is situated in Eastern part of the Central Iran. Tabas is a town with approximately 30,000 inhabitants, 950 kilometers southeast of Tehran, in the province of Yazd. This city was also hit by a major destructive earthquake on September 16th, 1978, during which about 22,000 persons lost their lives. The recorded earthquake magnitude was between 7.5 and 7.9 in the Richter scale. Despite major tectonic hazard concern in the Tabas region, relatively few studies attempted to analyses the local scale seismotectonic stress regime. For this reason in this paper we aim at characterising the stress regime that controls most earthquakes in this area through an inversion of the focal mechanisms of earthquakes.

**Analysis Method:** The inverse method adopted in this analysis reveals the stress state that best accounts for a set of double couple focal mechanisms of earthquakes, with no a priori choice between the nodal planes [2]. The stress tensor is reduced to four unknowns, because sole consideration of shear stress orientations cannot give access to isotropic component and scale factor of stress [3]. These four unknowns refer to the orientations of the three principal stress axes ($\sigma_1$, maximum compressive stress; $\sigma_2$, intermediate stress and $\sigma_3$, minimum stress) and the ratio of principal stress differences, $\Phi = [\sigma_2-\sigma_3]/[\sigma_1-\sigma_3]$.

This method involves consideration of the SSSC criterion (slip shear stress component). The SSSC is the component of stress acting in the slip direction of a fault. The intrinsic characteristics of the criterion adopted result in two main technical properties of the method [2]. First, no choice between the nodal planes is needed prior to or during the inversion. Second, the numerical aspects are reduced to a minimum so that the runtime is negligible regardless of the size of the data set.

**Corresponding Author:** Behzad G. Zamani, Department of Geology, Faculty of Natural Sciences, University of Tabriz, Iran
Tel: +98 411 3392700, Fax: +98 411 4448914 +98 711 2284572

Table 1: Focal mechanisms used to determine the regional stress in this study. These mechanisms are shown in the map of Fig. 1b, with the usual `beachball' presentation (Schmidt's type stereoplots with tension dihedral in black and pressure dihedral in white). Date (yyyymmdd) and time (hhmmss) follow usual convention and all angles are in degrees. Magnitudes of earthquakes (M) determined by body waves. For each focal mechanism, the two nodal planes are characterized by the strike (str), the dip (dip), the pitch of the inferred motion vector (pit) with letters indicating North (N), East (E), South (S) or West (W) and the sense (S) of relative motion with S for left lateral, N for normal, D for right lateral and I for reverse. The last column refers to the source of focal mechanism (see text)

| | | | | | | | *N.P.1* | | | | *N.P.2* | | | | |
|---|---|---|---|---|---|---|---|---|---|---|---|---|---|---|---|
| *.No.* | *Date* | *Time* | *Lat* | *Lon* | *Dkm* | *Mb* | *S* | *Strk* | *Dip* | *Pit* | *S* | *Strk* | *Dip* | *Pit* | *Source* |
| 1 | 19680901a | 072700 | 34,04 | 58,22 | 15 | 5,9 | N | 117 | 84S | 50W | D | 20 | 40E | 9N | N |
| 2 | 19680901b | 072730 | 34,04 | 58,22 | 15 | 5,9 | N | 18 | 36E | 46N | R | 148 | 65W | 63N | M |
| 3 | 19680901c | 191637 | 34,16 | 58,24 | 20 | 4,8 | N | 153 | 26E | 73S | R | 172 | 65W | 82S | MOS |
| 4 | 19740617 | 072249 | 33,66 | 57,01 | 35 | 4,8 | S | 123 | 48N | 41E | R | 3 | 61W | 50S | B |
| 5 | 19780916b | 153113 | 33,37 | 57,02 | 11 | 6,5 | R | 148 | 33E | 73N | R | 128 | 59S | 79W | CMT |
| 6 | 19780916c | 153556 | 33,37 | 57,44 | 0 | 6,4 | S | 61 | 64N | 22W | D | 161 | 70E | 28S | MOS |
| 7 | 19780916a | 153500 | 33,37 | 57,44 | 33 | 6,5 | R | 162 | 31E | 56N | R | 124 | 65S | 71W | B |
| 8 | 19780917a | 081723 | 33,65 | 57,02 | 25 | 4,9 | S | 4 | 52E | 45S | R | 62 | 56N | 48W | MOS |
| 9 | 19780917b | 124322 | 34,19 | 57,50 | 2 | 4,7 | S | 145 | 82W | 4S | D | 56 | 86N | 8E | MOS |
| 10 | 19781012 | 150142 | 33,39 | 57,42 | 18 | 4,9 | S | 50 | 75N | 16W | D | 144 | 75E | 16S | MOS |
| 11 | 19781206 | 171812 | 33,29 | 57,15 | 19 | 5,3 | S | 58 | 63N | 4W | D | 150 | 86E | 27S | MOS |
| 12 | 19790213 | 103600 | 33,32 | 57,43 | 33 | 5,5 | D | 157 | 35E | 40N | R | 102 | 68S | 62W | B |
| 13 | 19790213 | 103615 | 33,35 | 57,44 | 23 | 5,4 | R | 162 | 21E | 55N | R | 125 | 73S | 78W | MOS |
| 14 | 19800112 | 153141 | 33,49 | 57,19 | 33 | 5,4 | R | 172 | 32E | 49N | R | 126 | 66S | 68W | B |
| 15 | 19810430 | 102128 | 33,24 | 57,21 | 39 | 4,7 | S | 113 | 83N | 41W | D | 29 | 49E | 9S | MOS |
| 16 | 19870720 | 164746 | 33,82 | 56,99 | 16 | 5,0 | N | 117 | 79N | 63W | D | 48 | 29S | 23W | MOS |
| 17 | 19870830 | 055750 | 33,34 | 57,11 | 12 | 4,7 | S | 134 | 84S | 4W | D | 44 | 86E | 6N | MOS |
| 18 | 19880904 | 232458 | 33,99 | 58,24 | 15 | 5,0 | R | 146 | 65W | 89S | R | 144 | 25E | 88S | CMT |
| 19 | 19900325 | 000111 | 33,34 | 56,99 | 15 | 4,9 | D | 43 | 89W | 1S | S | 133 | 89N | 1E | CMT |
| 20 | 19901015b | 190652 | 33,71 | 56,84 | 26 | 4,9 | S | 69 | 50N | 28W | D | 178 | 69E | 44S | MOS |
| 21 | 19901015a | 190851 | 33,56 | 56,74 | 15 | 4,9 | R | 114 | 45S | 58W | R | 155 | 53E | 62N | CMT |
| 22 | 19680901 | 191637 | 34,16 | 58,24 | 20 | 4,8 | N | 153 | 26E | 73S | R | 172 | 65W | 82S | MOS |
| 23 | 19730511 | 135206 | 33,41 | 57,48 | 22 | 5,1 | S | 57 | 82N | 11W | D | 149 | 79E | 8S | MOS |
| 24 | 19740617 | 072206 | 33,73 | 57,11 | 24 | 4,7 | R | 7 | 51E | 46S | R | 64 | 56N | 49W | MOS |
| 25 | 19790117 | 032906 | 33,74 | 57,09 | 3 | 5,1 | S | 107 | 45N | 28E | R | 176 | 71W | 49S | MOS |
| 26 | 19790527 | 064306 | 33,23 | 57,24 | 11 | 4,6 | S | 97 | 30N | 14E | R | 175 | 83W | 61S | MOS |
| 27 | 19791202 | 061006 | 33,66 | 57,15 | 16 | 4,7 | N | 95 | 54N | 45W | N | 35 | 55E | 46S | MOS |
| 28 | 19830503 | 133006 | 33,27 | 57,37 | 31 | 4,7 | N | 155 | 75W | 65S | D | 94 | 29N | 32E | MOS |

Teble 2: Numerical results of the direct inversion to determine stress tensors, for the East-Central Iran. ωacc, threshold value adopted after application of refining process, for the inversion criterion ω (ranging from -100% for total misfit to 100% for perfect fit). In agreement with average estimated uncertainties in earthquake focal mechanisms, the stage with a 40% threshold value of ω has been adopted, except when identical rejection rate provides a better value, 45% or 50%. Nacc, number of accepted earthquake focal mechanisms. Nrej, number of rejected earthquake focal mechanisms (data with values of ω lower than 40 %). Stress axes σ1, σ2 and σ3 (maximum compressive, intermediate and minimum principal stress, respectively) with orientation given as trend and plunge in degrees. Φ, ratio of principal stress differences as defined by Angelier (1975 and 1989): Φ=(σ2-σ3)/(σ1-σ3). ωmoy and ωsd, average a posteriori estimator ω (from -100%, total misfit, to 100%, perfect fit) and standard deviation, as percentages. Auxiliary estimators: τ*moy and τ*sd for the average shear stress as percentage of maximum shear stress (0% to 100%) and its standard deviation, in percentages, αmoy and αsd for the average angle between observed slip and calculated shear stress, in degrees. These average estimators are calculated in the absence of any choice between nodal planes. Detailed explanation of the method in Angelier, 2002.

| $\omega_{acc}$ | $N_{acc}$ | $N_{rej}$ | $\sigma_1$ | | $\sigma_2$ | | $\sigma_3$ | | $\Phi$ | $\omega_{moy}$ | $\omega_{sd}$ | $\tau^*_{moy}$ | $\tau^*_{sd}$ | $\alpha_{moy}$ | $\alpha_{sd}$ |
|---|---|---|---|---|---|---|---|---|---|---|---|---|---|---|---|
| 40 | 20 | 8 | 242 | 20 | 143 | 21 | 11 | 60 | 0.22 | 77 | 19 | 84 | 15 | 19 | 15 |

**Data Sources:** Prior to our stress inversion in the East-Central Iran, we performed a detailed compilation of available double couple focal mechanisms of earthquakes in Iran. Focal mechanism solutions were obtained from a variety of sources. Some of these sources can be found in on-line moment tensors catalogs such as CMT [4] (Centroid Moment Tensor), available online at: http://www.seismology. harvard.edu/CMT search. Html (CMT symbol in Table 1) and MOS [5], available online at: http://wwwbrk.adm.yar. ru/russian/1 512/1 512 3e.html (MOS symbol in Table 1). Other sources were found from the literature, including Nowroozi [6], McKenzie [7] and Berberian [8], (N, M and B respectively in Table 1).

The source heterogeneity raised problems while building the data set. It was necessary to gather data from various sources because no technically homogeneous data set was available. In Iran, one must collected focal mechanism solutions from several moment tensor catalogues and papers to reach data numbers acceptable for stress inversion. Therefore, we collected data from several sources and built a database for Iran, [8] including the studied area. From the technical point of view, the construction of the database was not trivial because data

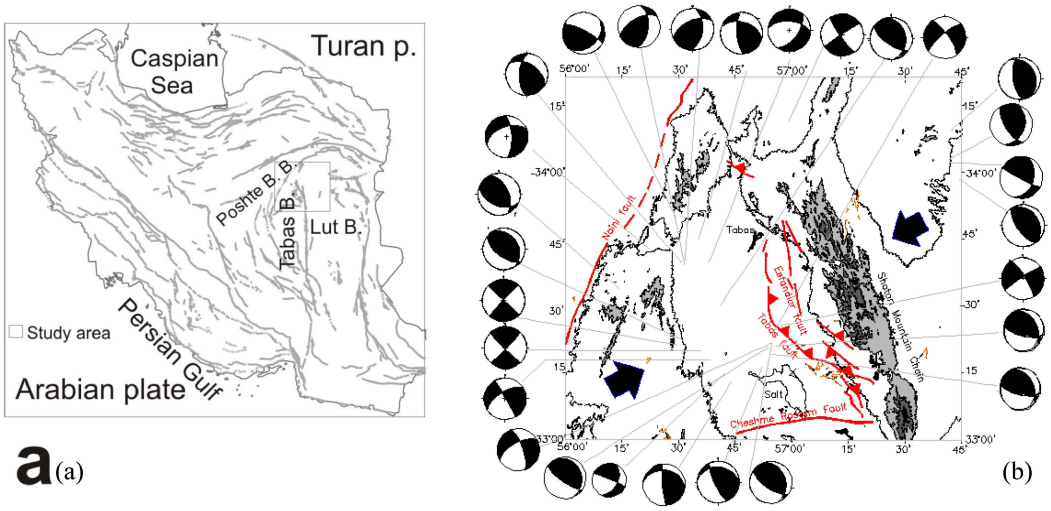


Fig. 1: Location map and focal mechanisms of earthquakes, in the East-Central Iran. Small steroplots as `beachball' illustration of double couple focal mechanisms (Schmidt's projection, lower hemisphere, tension and pressure dihedra respectively black and white). The frame of studied area is located in the map of Iran in the upper right part of the map. Major fault zones shown as thick lines in both maps adapted from Hessami *et al*. (2003). Results of the direct inversion method to determine average stress tensors, stress axes σ1 (maximum compressive principal stress) as pair of arrows indicate corresponding trends of compression. Numerical parameters given in Table 2.

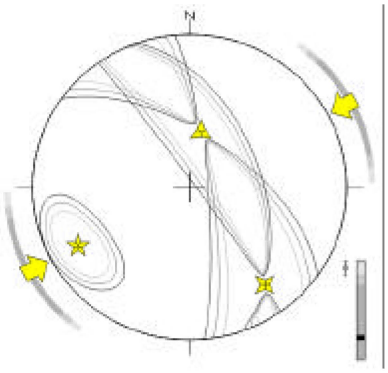


Fig. 2: Graphic results of the direct inversion to determine average stress tensors according to Angelier's method (2002), for this area analysed in the East-Central Iran. Stereoplot with Schmidt's projection of lower hemisphere. Stress axes σ1, σ2 and σ3 (maximum compressive, intermediate and minimum principal stress, respectively) as 5, 4 and 3-branch stars respectively, with confidence ellipses (60, 75, 90 %). Pair of arrows indicate corresponding trends of compression, with azimuth uncertainties in grey levels. Φ value and its uncertainties added as a scale bar (from 0 to 1) in lower-right corner of stereoplot.

from different sources had different formats, some of which were not explicit in terms of nodal planes strike, dip, slip and so on.

More important, in many cases contrasting solutions existed for the same earthquakes. Depending on the geometrical information provided by various authors, we examined the consistency of all proposed mechanisms in terms of nodal planes as well as individual *P*, *T* and *B*-axes. In some cases, we had to correct angular unconsistencies (such as for non-perpendicular nodal planes). The reliability of the fault plane solutions was evaluated in agreement with the values -when determinable- of the standard errors of *P* and *T*-axes orientations.

From this compilation, two or more focal mechanisms from different sources were commonly available for a single earthquake. In some cases, the proposed mechanisms could be regarded as identical within the range of data uncertainties. In other cases, they displayed significant differences in terms of nodal plane orientations. We consequently had to perform a critical comparison and select the most likely solution based on the techniques employed by authors and the accuracy and number of data used to determine each focal mechanism, when indicated.

Table 1 shows a summary of sources that reported focal solutions. For more details about the original data, the reader is referred to the source papers mentioned in the reference list. The focal mechanisms that we have consequently selected and used to determine the regional

stress are shown in Table 1 and the map of Figure 1b, with the usual 'beachball' presentation (that is, Schmidt's type stereoplots with tension dihedral in black and pressure dihedra in white).

**Results of Stress Analysis:** The results of stress inversion analysis in the East-Central Iran are summarised in Figure 1b and Figure 2. The numerical expression of the main results of the inversion is shown in Table 2. In Figure 1b, pair of arrows indicate the trends of compression resulting from the application of the direct inversion. In Table 2, some major parameters of the direct inversion have been added. Especially, $\omega_{acc}$ is the threshold value adopted after application of a specific refining process (see detailed explanation in Angelier, [2]). This value corresponds to the variable bound chosen for the inversion criterion $\omega$ (ranging from -100% for total misfit to 100% for perfect fit). In agreement with average estimated uncertainties in earthquake focal mechanisms, the stage with a 40% threshold value of $\omega$ has been adopted.

Accordingly, $\omega_{moy}$, is the average a posteriori estimator $\omega$ and $\omega_{sd}$ being its standard deviation. Auxiliary estimators are $\tau^*_{moy}$ for the average shear stress as percentage of maximum shear stress (0% to 100%, with $\tau^*_{sd}$ as standard deviation) and $\alpha_{moy}$ for the average angle between observed slip and calculated shear stress (in degrees, with $\alpha_{sd}$ as standard deviation). As a consequence of the moderate fit demand of 40%, the number of accepted earthquake focal mechanisms, $N_{acc}$, is large with respect to the number of considered focal mechanisms. $N_{rej}$, is the number of rejected earthquake focal mechanisms, that is, the number of data with a posteriori fit values $\omega$ lower than 40 %. The other numerical results include the trends and plunges of the stress axes $\sigma_1$, $\sigma_2$ and $\sigma_3$ and the ratio $\Phi$.

## DISCUSSION AND CONCLUSION

Determination of a consistent average state of stress, based on available focal mechanisms of earthquakes recorded from 1968 to 2009, acquire tectonic stress in the East-Central Iran region. The average stress is characterised by a NE-SW direction of compression (maximum compressive stress $\sigma_1$), the minimum stress axis being close to vertical and the calculated stress regime thus indicates a dominating thrusting mode. The number of earthquakes with dominating reverse mechanisms is 16, (57% of the data) and $\Phi$ is low, with a value of 0.22 indicating a rather small difference between $\sigma_2$ and $\sigma_3$ as compared with $\sigma_1$.

The dominating reverse-type stress is consistent with the evidences of reverse faults and focal mechanisms in this region. Because $\Phi$ is low, this stress regime does not contradict the presence of strike-slip active faults and focal mechanisms of earthquakes. Note, however, that because a moderate fit demand has been adopted a single average stress could be determined. Adopting a higher fit demand may result in a separation between different stress regimes corresponding to different reverse and strike-slip subsets of data. However, this was not done in the present paper for three reasons. (1) In the first approximation a single major stress regime accounts for the whole set of data from the East-Central Iran; (2) the number of focal mechanisms presently available in the study area is not large enough to ensure significant separation; (3) considering the relatively low angular accuracy of many ancient focal mechanisms, a separation into two or more sub-regimes with little contrast would be questionable.

The NE-SW compression stress reconstructed herein(trend N62°E) is not consistent with the direction of convergence (N˜10-34°E, NUVEL-1 and N21E, NUVEL-1A) indicated by both the latest plate kinematic reconstructions [12,13] and the recent geodetic GPS studies [14,15]. Also the results of Masson *et al.*, [16] that define the style of deformation by combined analysis of the geodetic strain-rate field and the strain-rate field deduced from the seismicity slightly consistence with stress analysis results. These inconsistencies locally, might be a result of the plates convergency and their kinematics. It is important, note that the present determination of seismotectonic compressive stress and the kinematic determinations in the same region are fully independent. It is worth nothing that our results indicate a local stress field between two micro-continent blocks, Tabas and East-Iran, not a regional stress field representing the general plate convergence. Our results are also compatible with the results of Mckenzie [17] and Jackson and McKenzie [18] regarding the convergence across Iran, between Eurasia and Africa-Arabia.

In the study area, Walker *et al.* [1] and Walker and Jackson, [19] considered major strike slip faults, such as the Naiband and Cheshme Rostam Faults (in our study area) ending into thrust faults (Tabas and Esfandiar faults) with WNW-ESE direction, along which the displacement is diminishing and often fail to reach the surface. Such blind faults are typical of the compressive deformation style in the East Iranian blocks. Shortening components associated with the strike-slip faults result in widespread thrust faulting. It seems our reconstructed compressive stress direction in this study, SW-NE, is responsible for reactivation of these faults.

Sarkar *et al*. [20] analysed sub-events of the Tabas earthquake and claimed that the fault plane solutions of earthquakes generally show WNW-ESE strikes, sub-parallel to the regional strike of the documented main fault systems. Also they concluded that the preferred fault planes corresponding to the main and the following sub events strike ESE-WNW, dip at steep angles and exhibit predominantly reverse thrust motion with some left-lateral strike-slip component. Such a slip process and our reconstructed stress direction are in conformity with a northwesterly propagating rupture initiated at the base of a listric thrust faults.

Earthquakes in NE-Iran [21] and in East-Central Iran are often associated with concealed Quaternary thrust faults located at the base of a series of low hills of Neogene clay deposits that separate the Shotori fold-thrust mountain belt to the east from the Tabas plain to the west [20]. Accordingly, body-wave seismograms for two earthquakes in September 1968 near Ferdows, 150 km east of Tabas, indicated thrust faulting at depths of about 10 km [1]. The identification of the stress direction in activation of thrust faulting is important for earthquake hazard assessment and also for an understanding of the local tectonics. One of the important results of our study is that the activity of concealed Quaternary thrust faults in East-Central Iran is controlled by the NE-SW direction of compression that we reconstructed by stress analysis in this study [22].

## ACKNOWLEDGEMENTS

The work was supported by the Centre of Excellence for Environmental Geohazards and the Research council of Shiraz University, the Ministry of the Sciences, Research and Technology of Iran, the Tabriz University.

## REFERENCES

1. Walker, R., J. Jackson and C. Baker, 2003. Surface expression of thrust faulting in eastern Iran: source parameters and surface deformation of the 1978 Tabas and 1968 Ferdows earthquake sequences, Geophys. J. Int. 152: 749-765.
2. Angelier, J., 2002. Inversion of earthquake focal mechanisms to obtain the seismotectonic stress (a new method free of choice among nodal planes) IV, Geophys. J. Int., 150: 588-609.
3. Angelier, J., 1984. Tectonic analyses of fault slip data sets., J. Geoph. Res., 89(B7): 5835-5848.
4. CMT, Centroid Moment Tensor catalogue, Harvard University, 2006. available online at:http://www.seisinology.harvard.edu/ CMT search.html
5 Mostriouk, A.O. and V.A. Petrov, 1994. Catalogue of focal mechanisms of Earthquakes 1964-1990, Materials of World Data Center B., Moscow, pp: 87. available online at http://wwwbrk.adm.yar.ru/rusian/1-512/1-512-3e.htm
6. Nowroozi, A.A., 1972, Focal mechanisms of Earthquakes in Persia, Turkey, West Pakistan and Afghanistan and plate tectonics of the Middle East, Bull. Seismol. Soc. Am., 62: 823-850.
7. McKenzie, D., 1972. Active tectonics of the Mediterranean region, Geophy. J.R. Astr. Soc., 30: 109-185.
8. Berberian, M., 1976, Contribution to the Seismotectonics of Iran (Part 10, Geological Survey of Iran, Rep., 39: 518.
9. Angelier, J., 1975. Sur l'analyase de measures recueillies des sites failles: l'utillite d'une confrontation entre les methods dynamiques et cinematiques, C. R. Hebd. Seanc. Acad. Sci. Paris D, 281: 1805-1808.
10. Angelier, J., 1989. From orientation to magnitudes in paleostress determinations using fault slip data, j. Str. Geo., 1/2: 37-50
11. Hessami, K., F. Jamali and H. Tabasi, 2003. Major Active Faults map of Iran, Scale 1:2500000, International Institute of Earthquake Engineering and Seismology (IIEES), 1 Sheet.
12. DeMets, C., R.G. Gordon, D.F. Argus and S. Stein, 1990. Current plate motions, Geophys. J. Int., 101: 425-478.
13. DeMets, C., R.G. Gordon, D.F. Argus and S. Stein, 1994. Effect of recent revisions to the geomagnetic reversal time scale on estimates of current plate motions, Geophys. Res. Letters., 21(20): 2191-2194.
14. Nilforoushan F., F. Masson P. Vernant, C. Vigny, J. Martinod, M. Abbasi, H. Nankali, D. Hatzfeld, R. Bayer, F. Tavakoli, A. Ashtiani, E. Doerflinger, M. Daignieres P. Collard and J. Chery, 2003. GPS network monitors the Arabia-Eurasia Collision deformation in Iran, J. Geodesy, 77: 411-422.
15. Vernant, P.H., F. Nilforoushan, D. Hatzfeld, M.R. Abbasi, C. Vigny, F. Masson, H. Nank-ali, J. Martinod, A. Ashtiani, F. Tavakoli and J. Chery, 2004. Present-day crustal deformation and plate kinematics in the Middle East constrained by GPS measurements in Iran and northern Oman, Geophys. J. Int., 157: 381-398.

16. Masson, F., J. Chery, D. Hatzfeld, J. Martinod, P. Vernant, F. Tavakoli and M. Ghafory-Ashtiani, 2005. Seismic versus aseismic deformation in Iran inferred from earthquakes and geodetic data. Geophys. J. Intl., 160: 217-226.
17. McKenzie, D., 1972. Active tectonics of the Mediterranean region, Geophy. J. R. Astr. Soc., 30: 109-185.
18. Jackson, J.A. and D.P. McKenzie, 1984. Active tectonics of the Alpine-Himalayan belt between western Turkey and Pakistan, Geophys. J. R. Astr. Soc., 77: 185-264.
19. Walker, R. and J. Jackson, 2004. Active tectonics and Late Cenozoic strain distribution in central and eastern Iran, Tectonics, 23, TC5010, doi:10.1029/2003TC001529.
20. Sarkar, I., V. SriRam, H. Hamzehloo and K.N. Khattri, 2005. Subevent analysis for the Tabas earthquake of September 16, 1978, using near field accelerograms. doi:10.1016/j.pepi.2005.01.004.
21. Zamani, Behzad G., Angelier Jacque and Zamani Ahmad, 2008. State of stress induced by plate convergence and stress partitioning in northeastern Iran, as indicated by focal mechanisms of earthquakes, J. Geodynamics, 45: 123-130.
22. Zamani, G. and Behzad, 2009, State of Tectonic stress in Iran, Ph.D. thesis, Shiraz University, pp: 120.